Methodology for Flow and Salinity Estimates in the Sacramento-San Joaquin Delta and Suisun Marsh

32nd Annual Progress Report
June 2011

Chapter 5
Adaptive Mesh, Embedded Boundary Model for Flood Modeling

Authors: Qiang Shu and Eli Ateljevich,
Delta Modeling Section,
Bay-Delta Office,
California Department of Water Resources

Contents

Figures

5 Adaptive Mesh, Embedded Boundary Model for Flood Modeling

5.1 Summary

We describe a 2-dimensional shallow water model designed to simulate water quality and flooding. The model uses a finite-volume discretization of the shallow water equations on an adaptive Cartesian mesh, using embedded boundaries to represent complex topography. For flooding applications, we use adaptive mesh refinement (AMR) to evolve Cartesian sub-grids near a flood front, which leads to a resolved local result. Fluxes on the front itself are described using wet-dry Riemann solutions. The algorithms are implemented in parallel and highly scalable. The model is tested using analytical solutions of flood propagation on wet and dry channels and of a dam-break problem. Applications to flooding in arbitrary bathymetry are discussed.

5.2 Introduction

The California Department of Water Resources (DWR) and Lawrence Berkeley National Laboratory (LBNL) are collaboratively developing a multi-dimensional computer model to solve the shallow-water equations. The motivation of the project is to provide a high performance, accurate, and open-source tool for decision making support in the San Francisco Bay and Sacramento-San Joaquin Delta. The Bay-Delta system is a nexus of water policy debate and scientific scrutiny, with constantly shifting concerns including salt intrusion, fish and pollutant transport, water supply reliability, and flooding of Delta islands. In particular, the property and infrastructure risk posed by flood events underscores the need for models in flood risk assessment and planning.

Our shallow water model REALM (River, Estuary, and Land Model) includes a shock-capturing algorithm and 2 technologies relevant to flood modeling: adaptive mesh refinement and embedded boundaries. We employ adaptive mesh refinement (AMR) [(Berger and Oliger 1984) (Berger and Colella 1989)] to refine fronts, maintain resolution at local length scales and concentrate computational resources on predefined areas of interest. We use a Cartesian mesh with embedded boundaries (EB) to represent the natural shoreline. Although adaptive mesh refinement has been used before in flood modeling [e.g. (George 2006); (Begnudelli, Sanders and Bradford 2008)], we believe that the use of AMR and EB together is novel, particularly in context of a scalable, parallel computer architecture.

This chapter summarizes our algorithm, describes details relevant to flood modeling, and describes the verification of our model for transient flooding events using problems from the literature on wet and dry beds. We discuss wet bed applications in a natural setting with arbitrary topography, as well as some of the challenges and ambiguities of the EB-AMR approach on 2 different types of wetting and drying problems.

5.3 Governing Equations

Our shallow water model REALM is based on the 2D depth-integrated Navier-Stokes equations, with a hydrostatic treatment of pressure, Boussinesq assumption concerning salt-induced horizontal (baroclinic) density variation and friction. The shallow water equations are commonly and efficiently used as models of flood propagation and inundation, a practice that is noted and critiqued in (Alcrudo 2002).

In terms of the height of the water column h, local velocities u and v and salt concentration s, the shallow water equations in conservation form are

$$\frac{\partial U}{\partial t} + \frac{\partial (F^x)}{\partial x} + \frac{\partial (F^y)}{\partial y} = S \qquad \text{Eq. 5-1}$$

where the conserved variable vector $U = (h, hu, hv, hs)^T$ and the flux across cell faces in x and y directions are

$$F^x = \begin{pmatrix} hu \\ hu^2 + \frac{g\rho h^2}{2\rho_0} \\ huv \\ hus \end{pmatrix} \qquad \text{Eq. 5-2}$$

$$F^y = \begin{pmatrix} hv \\ huv \\ hv^2 + \frac{g\rho h^2}{2\rho_0} \\ hvs \end{pmatrix} \qquad \text{Eq. 5-3}$$

In these equations, g denotes the gravitational constant, ρ_0 denotes the density of fresh water, and $\rho = \rho(s)$ is an equation of state. To focus on flooding and the hyperbolic component of our solver, viscous terms, including horizontal eddy diffusivity and salt dispersion are not discussed here.

The sources and sinks include pressure forces from the bed, friction stress, and other local sources of mass or momentum such as wind or Coriolis acceleration. Here we consider only bottom pressure and friction:

$$S = \left[0, -\frac{g\rho}{\rho_0} h b_x - \tau_x, -\frac{g\rho}{\rho_0} h b_y - \tau_y, 0 \right]^T \quad \text{Eq. 5-4}$$

where b_x and b_y are the slope of the bed in x and y direction and τ_x is a bottom stress given by the Chezy formula (Molls, Zhao and Molls 1998):

$$\tau_x = \frac{\rho}{\rho_0 C^2} u \sqrt{u^2 + v^2} \quad \text{Eq. 5-5}$$

$$\tau_y = \frac{\rho}{\rho_0 C^2} v \sqrt{u^2 + v^2} \quad \text{Eq. 5-6}$$

where C is the Chezy coefficient.

5.4 Solution Algorithm

We use a finite volume discretization of the shallow water equations, based on a Cartesian grid with embedded boundaries representing shorelines. Data are collocated at cell centers. Our algorithm is best articulated in 3 tiers:

AMR: Adaptive mesh refinement orchestrates integration over the multiple levels of grids refined in space and time.

EB: We use a special treatment on the cell containing shoreline.

Godunov: Single grid computations are handled by a second order Godunov scheme with corner transport upwind (CTU) treatment of fluxes at cell faces.

5.4.1 Adaptive Mesh Refinement

In the organization of our algorithm, adaptive mesh refinement plays the role of an outer controller, sequentially advancing the time step at different levels of refinement. The AMR component of our algorithm follows Berger and Colella (1989) as modified by Colella, Graves, et al. (2006) and Pember, et al. (1995) for embedded boundaries. The cycle of information is depicted in Figure 5-1. Levels of the AMR hierarchy are integrated from coarse to fine. Between levels, results in coarse cells abutting fine-coarse interfaces (dots) are used to help estimate boundary conditions for the next finer level. Upon completion of the time step, fine cell states and fine cell fluxes are averaged and used to replace data in underlying coarse cells. When regridding occurs, further interpolation is required to fill new levels. The result is a conservative, consistent estimate over the hierarchy. Our AMR approach allows flexible criteria for refining cells, including user-prescribed refinement, refinement based on (Richardson extrapolation) error estimates, presence of a wet-dry interface, or sharp gradients.

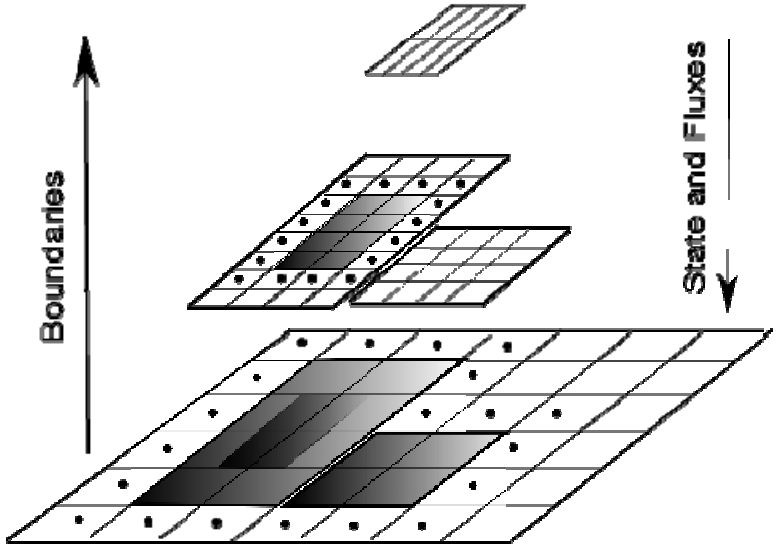

Note: Coarse cells adjacent to fine cells (dots) are used to provide boundary conditions for the fine mesh

Figure 5-1 A multiblock adaptive mesh hierarchy with a refinement factor of 2 between levels

5.4.2 Embedded boundaries

We use Cartesian cut cells (Colella, Graves, et al. 2006) to represent natural boundaries with high fidelity without a steep time step penalty in partial cells due to the use of an explicit integration method. Figure 5-2 shows a grid intersecting the boundary at a shoreline. The grid is decomposed into regular, irregular, and covered cells (covered cells are implied by elimination).

Regular cells are integrated using methods for a square Cartesian mesh. Irregular volumes of fluid are treated using a hybrid update that combines a conservative small cell estimate with a non-conservative full cell estimate, using weights proportional to the fraction of the irregular cell that is wet. The non-conservative divergence contributes stability; the conservative divergence preserves mass and momentum, induces the boundary condition, and is accurate. The combination induces a mass and momentum discrepancy, and the mismatch is mitigated by redistribution of the discrepancy to nearby cells. Further details are discussed in Colella, Graves, et al. (2006).

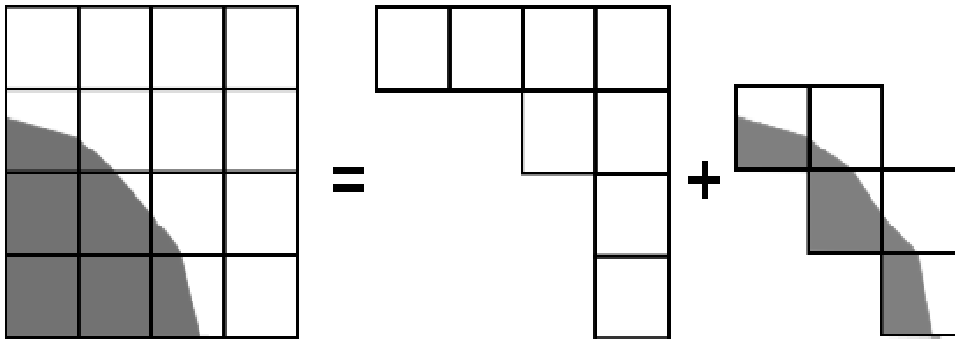

Note: Gray regions are outside the domain. Covered cells have been removed from the illustration on the right side.

Figure 5-2 Decomposition of a patch of cells into regular, irregular, and covered cells

5.4.3 Godunov algorithm

Within one multiblock grid, we employ the solution algorithm in Colella, Graves, et al. (2006), which is a finite volume predictor-corrector method: We construct accurate, upwinded estimates of the fluxes on cell faces and then update cell average values. The technique has the following attributes:

1. Calculation of spatial gradients using limiters to avoid oscillations near discontinuities.
2. Extrapolation in one space dimension and time of variables from cell centers to edge centers at the half time.
3. Solution of a Riemann problems for upwinding, which convert the dual estimates of extrapolated variables on each side of a face into upwinded fluxes. We use a primitive solver based on the linearized problem as described in Toro (2006). The solution is modified to include salinity-induced density variation.
4. Modification of the dual, one dimension estimate with fluxes in the transverse direction, as in the Corner Transport Upwind method of Colella (1990).

The algorithm produce upwinded fluxes and primitive variable estimates that are shock-capturing, second order accurate in smooth flow, and robust to flow oblique to the coordinate faces. In cells that

intersect the shore, the upwinded primitive variables are further interpolated and combined into a conservative divergence as described in the previous section.

Source terms are integrated using Heun's method. A well known difficulty with explicit finite volume representations is maintaining quiescent flow. The pressure component of the flux must be discretized in such a way to balance the bed pressure source in quiescent flow. Otherwise, the discretization can excite flow from a fluid at rest. Our characterization of bed pressure is based on this balance using a source discetization with face contributions analogous to the face contributions to the flux divergence under the conditions that the water surface is level (at the cell center level) and velocity is zero. Because the flux divergence is a hybrid, the bed source is too. The approximation is consistent with the source terms $-\frac{g\rho}{\rho_0} hb_x$ and $-\frac{g\rho}{\rho_0} hb_y$ in the original partial differential equation (PDE) and preserves quiescent flow well.

5.5 Wet/Dry Front Capture

In flood modeling, one of 2 treatments of an evolving flood front is usually adopted. The first, which is common for modeling tsunamis and intertidal mudflats, is to treat front propagation as a side effect of rising or falling water on bathymetry (Figure 5-3a). The second propagates the flood as a discontinuity (Figure 5-3b) and requires the ability to track or capture the evolving front.

The results we present here are for evolution over a flood plain. We use our hyperbolic algorithm, wet-dry Riemann solvers, and AMR to capture flood waves (Figure 5-3b). We use embedded boundaries to model shores that do not move. The capability to model the interaction between water levels and bathymetry (Figure 5-3a) is a work in progress.

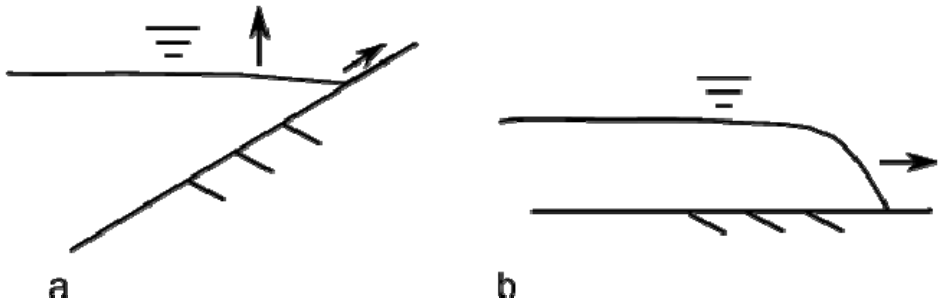

Figure 5-3 Two depictions of flooding

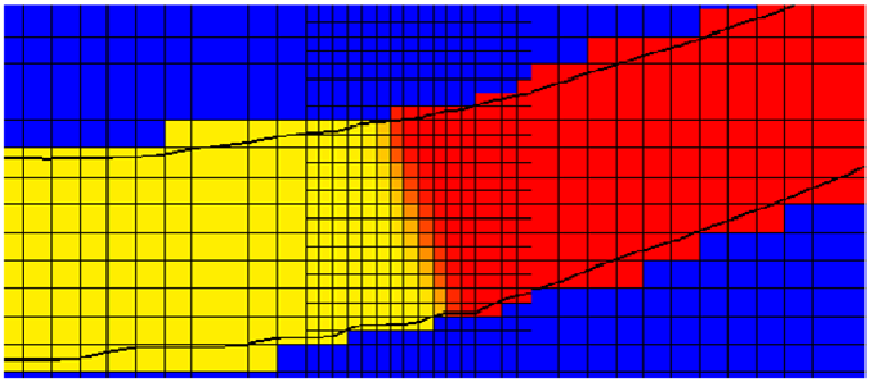

Figure 5-4 AMR resolving a flood along a reach of the Sacramento River

Adaptive mesh refinement is used to help resolve the flood wave front. Figure 5-4 shows subgrids spawned around a flood wave front on a reach of the Sacramento River based on the gradient of the solution. We also use dry-wet interfaces as a criterion for re-gridding. Embedded boundaries represent the (in this case, static) levee boundaries.

Due to the Godunov finite volume discretization, upwinding, and use of gradient limiters, our algorithm is inherently able to capture discontinuities such as flood waves and wet-dry fronts. In the Godunov algorithm, we estimate the state on the faces and switch between an exact wet/dry Riemann solution and approximate state wet/wet Riemann solution based on whether the faces are wet or dry. On faces with both sides dry, depth and velocity are of course always set to zero.

As will be seen in the next section, the model is capable of resolving and reproducing the shallow water physics of an advancing flood on both wet and dry beds.

5.6 Model Verification

We have applied our code to several flood and dam-break test cases proposed by CADAM (Concerted Action on Dam Break Modeling) to verify the stability and accuracy flood algorithms. A detailed description of the test suite is available in Goutal and Maurel (1997). Here we present results for CADAM tests 3, 4 and 5.

5.6.1 Dam Break on a Dry Bottom

This test problem has data containing a dry bed to the right of dam in a rectangular channel with a flat bottom. An instantaneous dam break is assumed, and unsteady flow velocity and water depth are computed by the model. An analytical solution (Ritter Solution) exists for the test and is given in Goutal and Maurel (1997). The objective of this test is to test the stability of the code in simulating the propagation of a wave over the dry zone.

The spatial domain is represented by a 2048x16 m rectangular cross section channel, which is discretized using 1 m square cells. The channel bottom is assumed frictionless and initial condition is set to:

$$\begin{cases} h = 6m, \quad u = 0 \quad \text{if} \quad x < 0 \\ h = 0m, \quad u = 0 \quad \text{if} \quad x > 0 \end{cases}$$

The dam break occurs at x=0. The time step is adapted to maintain a Courant number of 0.9. Results for this test are shown at time=50.78 s in Figure 5-5.

The simulated dry/wet surface matches the analytical solution well. In Figure 5-5 REALM correctly simulates the jump of velocity at the front without obvious oscillation.

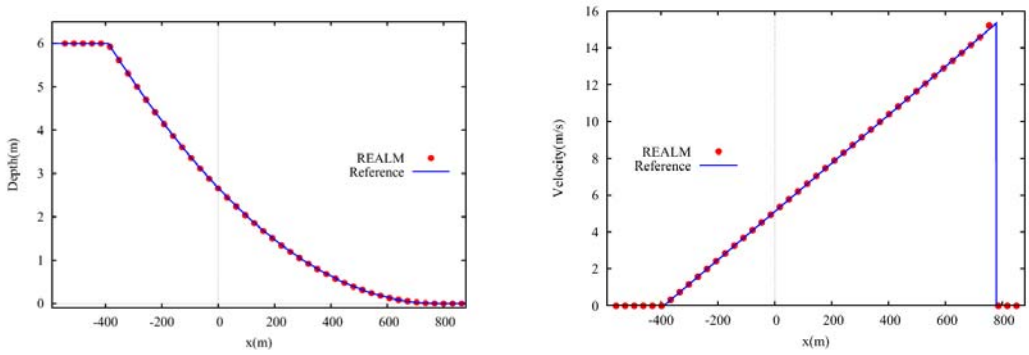

Figure 5-5 Water depth (left) and velocity (right) after dam break at time 50.78 seconds

5.6.2 Dam Break on a Wet Bottom

This test problem has data containing a wet bed to the right of dam in a rectangular channel with a flat bottom. An instantaneous dam break is assumed, and unsteady flow velocity and water depth are computed by the model. An analytical solution (Goutal and Maurel 1997) exists for the test. The objective of this test is to observe the ability of the code to resolve (a) the speed of wave propagation, (b) the strength of the jump on the shock front, (c) the width of the shock layer and (d) stability in the vicinity of the shock.

The spatial domain is again represented by a 2048x16 m rectangular cross section channel discretized using 1 m size square cells. The channel bottom is assumed frictionless and initial condition is set to:

$$\begin{cases} h = 6m, \quad u = 0 \quad \text{if} \quad x < 0 \\ h = 2m, \quad u = 0 \quad \text{if} \quad x > 0 \end{cases}$$

The dam is at x=0. The time step is adaptive to maintain a Courant number of 0.9.

Results for this test are shown at time 50.52 seconds in Figure 5-6.

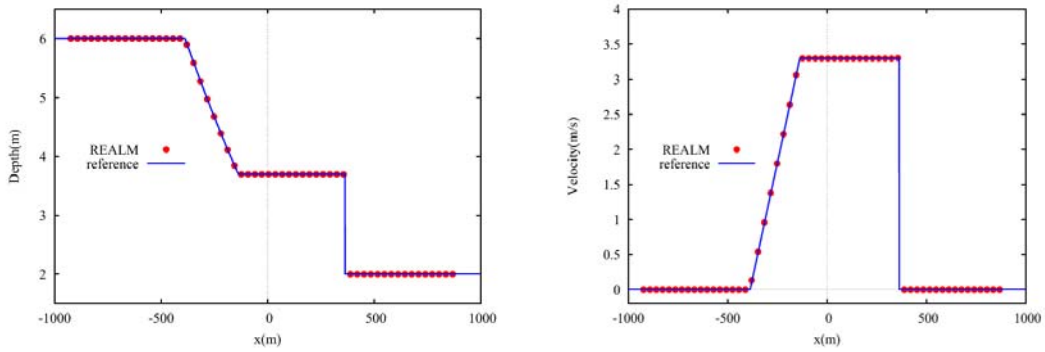

Figure 5-6 Water depth (left) and velocity (right) after dam break at time 50.52 seconds

Again REALM performs well with respect to the objectives of this test. The simulated left transonic rarefaction wave and right shock wave match their analytical counterparts as shown in Figure 5-6. The downstream wave moves faster than upstream wave, a feature of the analytical solution. In the left rarefaction wave, simulated water depth and velocity are smooth without any distinct break point. In the middle shock layer zone, both the computed water depth and velocity match the analytical solution well. There are no oscillations in the vicinity of the computed shock.

5.6.3 Dam Break on a Dry Bottom with Friction

In this test, REALM is applied to the unsteady flow resulting from an instantaneous dam breaking in a rectangular channel with constant width and with friction. Only the approximate Dressler solution (Dressler 1952) is available, the validity of which is limited to a region comprising less than one-third the distance to the point where the solution gives a zero value of flow. The objectives of this test are to validate the ability of the code to propagate a wave front over a dry bed with friction.

The spatial domain is again represented by a 2048x16 m rectangular cross section channel discretized using 1 m size square cells. The Chezy coefficient is set to 40 and the initial condition is set to:

$$\begin{cases} h = 6m, \quad u = 0 \quad \text{if} \quad x < 0 \\ h = 0m, \quad u = 0 \quad \text{if} \quad x > 0 \end{cases}$$

The dam is at x=0. The time step is adaptive to maintain a Courant number of 0.9.

Results for this test are shown at time 50.88 seconds in Figure 5-7.

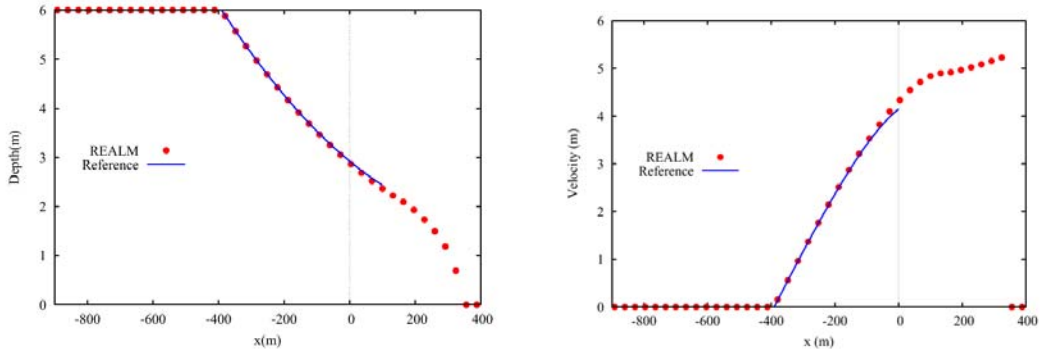

Figure 5-7 Water depth (left) and velocity (right) after dam break at time 50.88 seconds

The simulated result shows an apparent slowing down of the wave front. This effect is caused by the friction term. Upstream of the dam, REALM correctly computes water depth and velocity. The behavior of REALM is stable in the vicinity of the wave front.

5.7 Applications and Challenges

REALM appears to do well on a class of flood evolution problems involving flat bathymetry regardless of whether the bed is wet or dry. Anecdotally, we have observed that the model also handles practical flooding problems in fully wetted channels robustly. We point out, however, that the benchmarks presented in this paper focus on flat beds. This class of problem poses some of the greatest numerical challenges for flooding, but application of REALM on wetting and drying problems dominated by topography is still under development.

One problem during drying is caused by inaccurate reconstruction of volumes, depths, and face apertures in partially wet cells from the water surface. As a cell dries, its 2D area shrinks. The relationship between average depth and surface becomes more difficult to estimate. The cell can dry out early, and inconsistencies can develop between whether the cell is considered wet and whether a face is considered wet.

Begnudelli, Sanders, and Bradford (2008) noted similar problems and reconstruct the depth of partially dry faces by extrapolating a surface from the wet neighbors. Casulli (1990) proposes the use of a subgrid bathymetry model comprised of piecewise flat elements.

We are working to address the problem by updating the embedded boundary depiction of the domain along with fluctuations in the surface. On a domain with a steep bed, the treatment amounts to a subgrid bathymetry model. On a domain with a shallow bed slope, the flood front can move across the cell easily as a wave and be captured by the numerics, as was the case in the results presented here.

Another issue we have experienced is that high fluxes tend to overdraw the adjacent cells of mass and momentum. Sleigh et al. (1998) used a limited flux to solve this issue, in which momentum flux is set to zero and only mass flux is considered. Another solution in keeping with the mechanics of our algorithm is to include the overdraft as part of mass and momentum redistribution in the EB component algorithm, donating it to neighboring cells in proportion to the mass already contained in the cells. We also continue to hone our Riemann solutions for this application, as our approximate state Riemann solver is sometimes the source of unrealistic fluxes in extremely shallow flows.

5.8 Acknowledgements

Phillip Colella and Peter O. Schwartz of Lawrence Berkeley National Laboratory assisted with this investigation.

5.9 References

Alcrudo, F. "A state of the art review on mathematical modelling of flood propagation." *1st IMPACT Project Workshop.* 2002.

Begnudelli, L., B. F. Sanders, and S. F. Bradford. "Adaptive godunov based model for flood simulation." *J. Hydraul. Eng.* 34(6) (2008): 714–725.

Berger, M., and J. Oliger. "Adaptive mesh refinement for hyperbolic partial differential equations." *J. Comput. Phys.* 53 (1984): 484–512.

Berger, M., and P. Colella. "Local adaptive mesh refinement for shock hydrodynamics." *J. Comput. Phys.* 82(1) (1989): 64-68.

Casulli, V. "A high-resolution wetting and drying algorithm for free-surface hydrodynamics." *Int. J. Numer. Meth. Fluids* 60 (1990): 391–408.

Colella, P. "Multidimensional upwind methods for hyperbolic conservation laws." *J. Comput. Phys.* 87 (1990): 171–200.

Colella, P., D. T. Graves, B. J. Keen, and D. Modiano. "A cartesian grid embedded boundary method for hyperbolic conservation laws." *J. Comput. Phys.*, 2006: 347–366.

Dressler, R. F. "Hydraulic resistance effect upon the dam-break functions." *J. Res. Natl. Bur. Stand.* 49(3) (1952): 217–225.

George, D. "Finite volume methods and adaptive refinement for tsunami propagation and inundation." PhD thesis, University of Washington, 2006.

Ghidaglia, J. M., and F. Pascal. "On boundary conditions for multidimensional hyperbolic systems of conservation laws in the finite volume framework." *CMLA, ENS de Cachan.* 2002.

Goutal, N., and F. Maurel. "Description of the test cases." *Proceedings of the 2nd Workshop on Dam-Break Wave Simulation.* 1997. 18–28.

Molls, T., G. Zhao, and F. Molls. "Friction slope in depth-averaged flow." *J. Hydraul. Eng.* 124(1) (1998): 81-85.

Pember, R. B., J. B. Bell, P. Colella, and W. Y. Crutchfield. "An adaptive Cartesian grid method for unsteady compressible flow in irregular regions." *J. Comput. Phys.* 120(2) (1995): 278–304.

Sleigh, P. A., M. Berzins, P. H. Gaskell, and N. G. Wright. "An unstructured finite-volume algorithm for predicting flow in rivers and estuaries." *Computers & Fluids* 27(4) (1998): 479–508.

Toro, E. F. *Shock-Capturing Methods for Free-Surface Shallow Flows.* Chichester: John Wiley and Sons, 2006.